Figure S1: Glucose deprivation induces YAP Activation

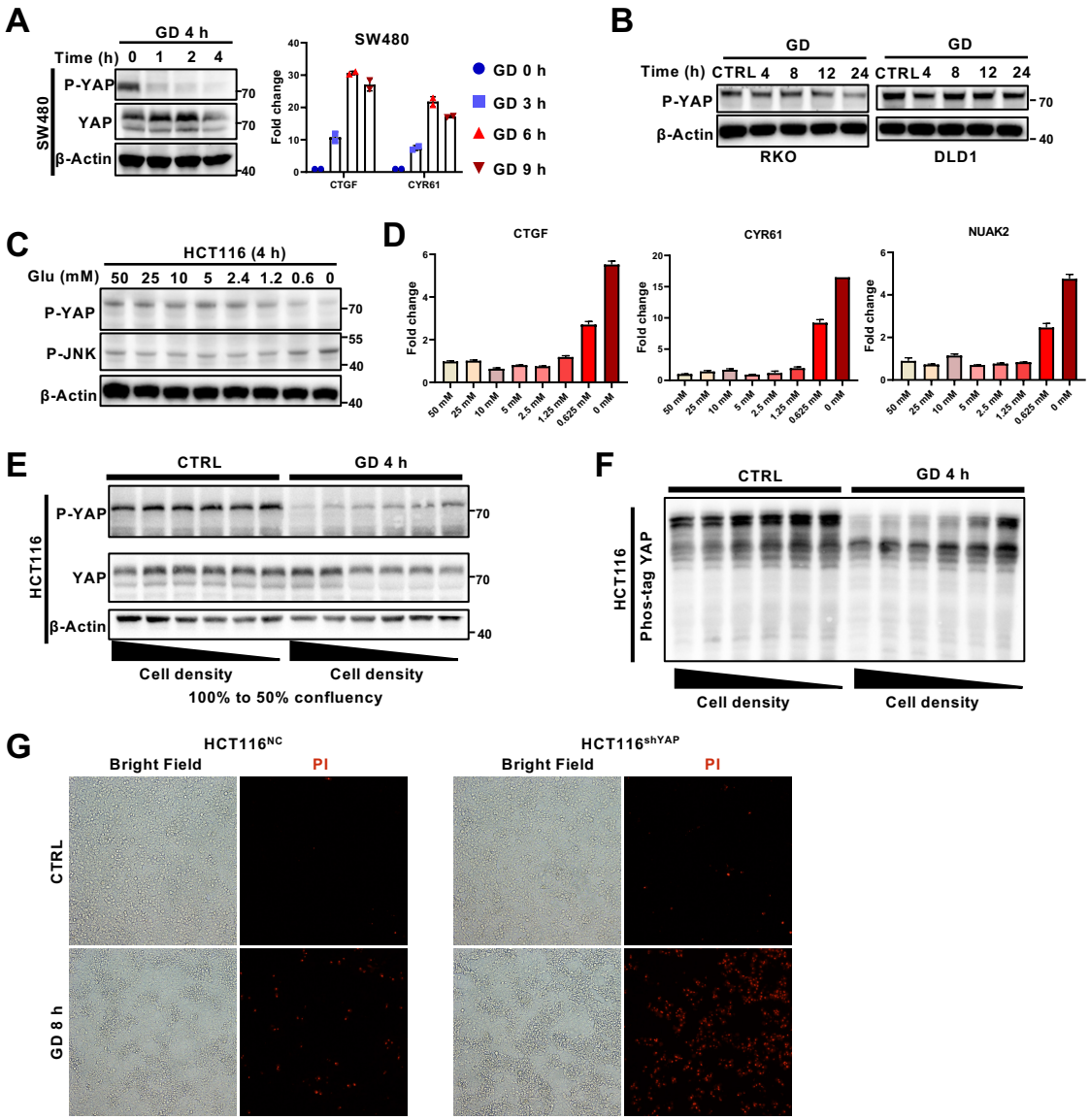

Figure. S1. Glucose deprivation induces YAP activation. Related to Figure 1.

(A) Immunoblotting (left) of YAP phosphorylation (serine 127) and RT–qPCR (right) of YAP target genes (*CTGF, CYR61*) in SW480 cells under GD for the indicated times.

(**B)** Immunoblotting of YAP phosphorylation (serine 127) in RKO cells (left) and DLD1 cells (right) under GD for the indicated times. Actin was used as a loading control.

(**C)** Immunoblotting of YAP phosphorylation (serine 127), JNK phosphorylation and EZH2 expression in HCT116 cells treated with the indicated doses of glucose for 4 h.

(**D)** RT–qPCR of YAP target genes (*CTGF, CYR61, NUAK2*) in HCT116 cells treated with the indicated doses of glucose for 3 h.

(**E)** Immunoblotting analysis of YAP phosphorylation (serine 127) and YAP in GD (0 mM, 4 h)-treated HCT116 cells with different confluence. Actin was used as a loading control.

(F) Phos-tag gel was used to examine YAP phosphorylation in the same samples in (E).

(G) PI staining of HCT116-NC and shYAP cells treated under normal conditions or GD (0 mM, 8 h).

Figure S2: Purine nucleoside supplementation rescues GD-induced YAP activation

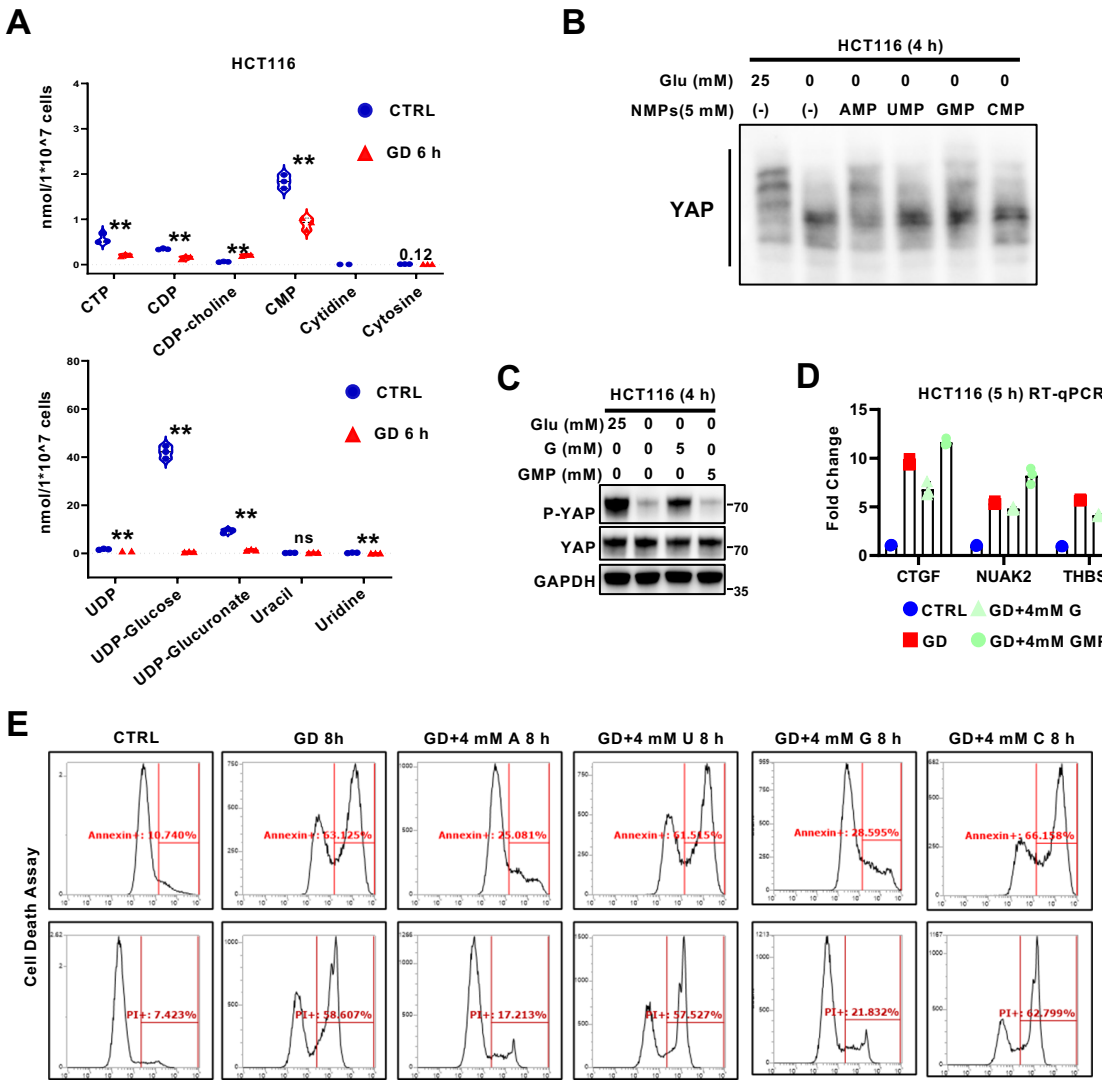

Figure. S2. Purine nucleoside supplementation rescues GD-induced YAP activation. Related to Figure 2.

(A) Levels of the metabolites involved in pyrimidine (cytosine and uracil) nucleotide metabolism in HCT116 cells under normal conditions and GD (0 mM, 6 h).

(B) Phos-tag gel showing YAP phosphorylation in HCT116 cells under normal conditions or GD (0 mM, 4 h) with or without AMP, UMP, GMP or CMP.

(C) Immunoblotting of YAP phosphorylation (serine 127) and YAP expression in HCT116 cells under normal conditions or GD (0 mM, 4 h) with or without G or GMP.

(D) RT–qPCR of YAP target genes (*CTGF, NUAK2* and *THBS1*) in HCT116 cells treated as in (C).

(E) FACS analysis of Annexin V/PI staining of HCT116 cells under normal conditions or GD (0 mM, 8 h) with or without A, U, G or C.

Figure S3: Ribose-phosphates attenuate GD-induced YAP activation

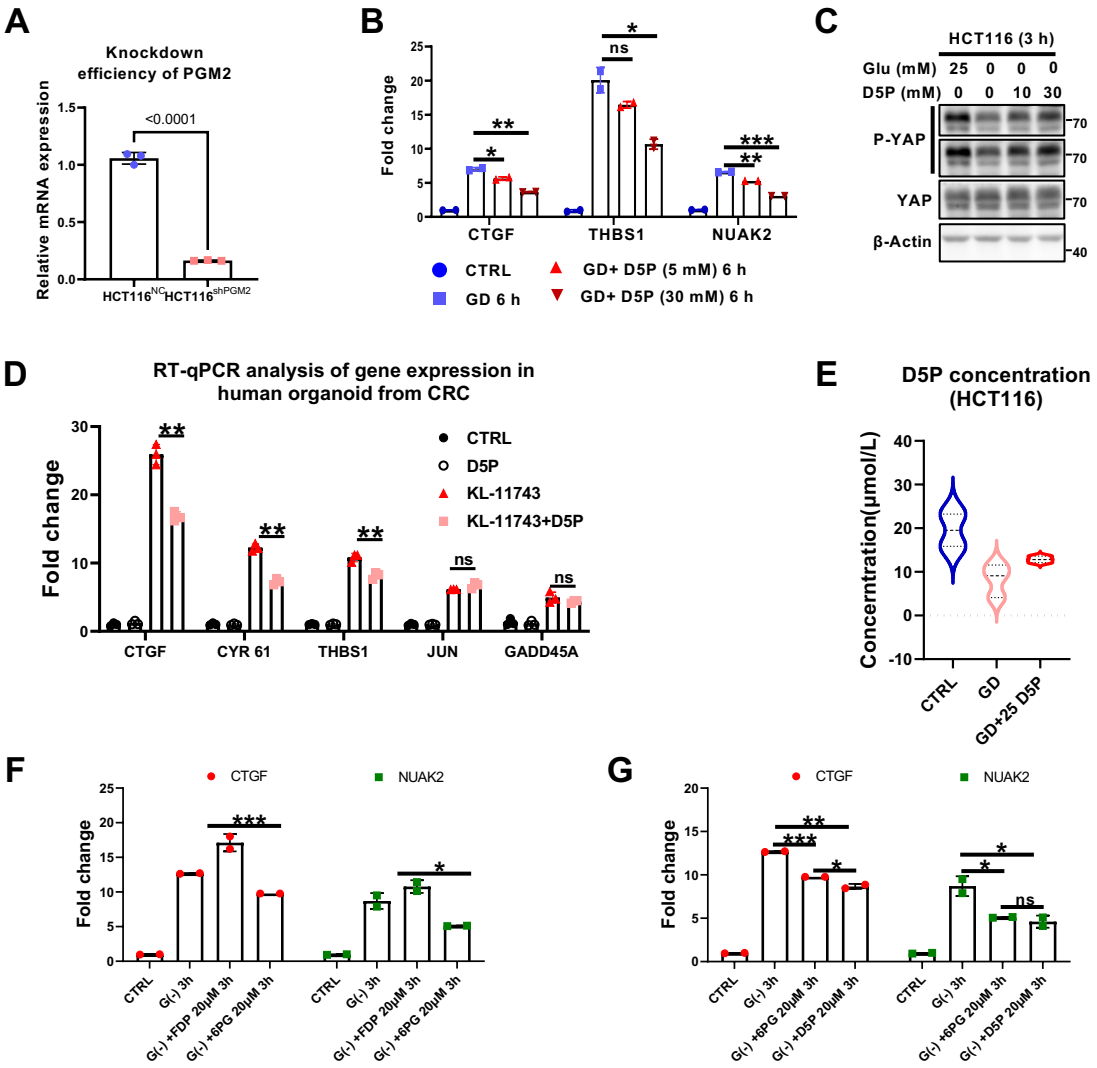

Figure. S3. Ribose-phosphates attenuate GD-induced YAP activation. Related to Figure 3.

(A) RT–qPCR analysis of knockdown efficiency of PGM2 in HCT116 cells.

(B) RT–qPCR of YAP target genes (*CTGF, CYR61* and *NUAK2*) in HCT116 cells under normal conditions or GD (0 mM, 6 h) with or without D5P.

(C) Immunoblotting of YAP phosphorylation (serine 127) and YAP expression in HCT116 cells under normal conditions or GD (0 mM, 3 h) with or without D5P. Actin was used as a loading control.

(D) RT–qPCR of YAP target genes (*CTGF, NUAK2* and *THBS1*) and JNK target genes (*JUN* and *GADD45A*) in CRC patient-derived organoids cultured under normal conditions or KL-11743 treatment (5 mM, 3 h) with or without D5P.

(E) D5P level in GD-treated HCT116 cell with or without D5P supplementation.

(F) RT–qPCR of YAP target genes (*CTGF* and *NUAK2*) in HCT116 cells under normal conditions or GD (0 mM, 3 h) with or without FDP or 6PG.

(G) RT–qPCR of YAP target genes (*CTGF* and *NUAK2*) in HCT116 cells under normal conditions or GD (0 mM, 3 h) with or without 6PG or D5P.

Figure S4: Guanosine-induced D5P up-regulation promotes LAST1 re-solubilization to inactivate YAP

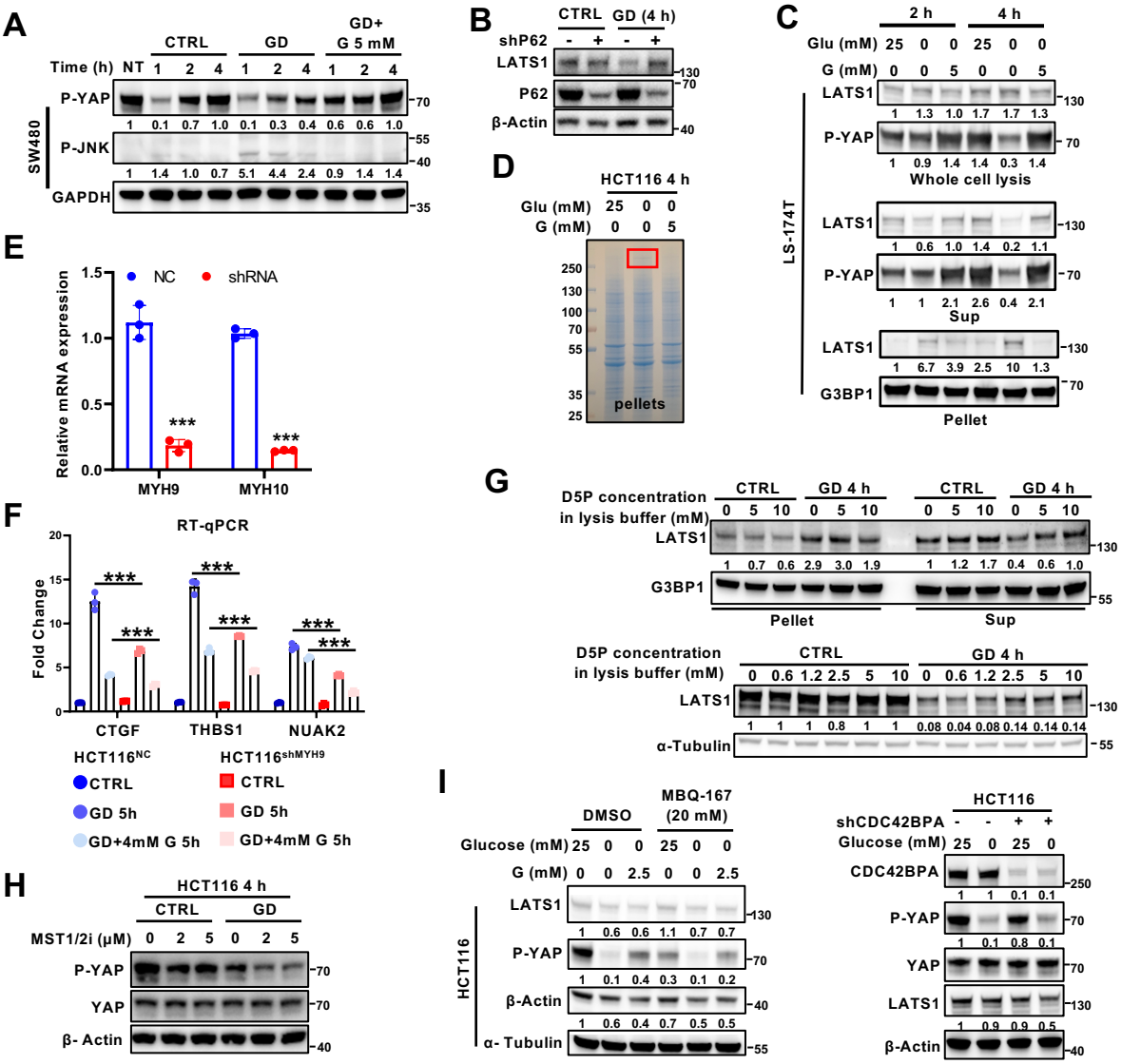

Figure. S4. Guanosine-induced D5P up-regulation promotes LATS1 re-solubilization to inactivate YAP. Related to Figure 4.

(A) Immunoblotting of YAP phosphorylation (serine 127) and JNK phosphorylation in SW480 cells under normal conditions or GD (0 mM) with or without G supplementation for the indicated times. GAPDH was used as a loading control.

(B) Immunoblotting of LATS1 and P62 expression in HCT116 NC and shP62 cells under normal conditions or GD. Actin was used as a loading control.

(C) Immunoblotting of LATS1 expression and YAP phosphorylation (serine 127) in the supernatants (Sup) and pellets of LS-174T cells under normal conditions or GD with or without G. G3BP1 was used as a loading control.

(D) Coomassie blue staining of the differential bands in the pellets of HCT116 cells under GD. The differential band marked in red was the same size as that in the LATS1-immunoprecipitated samples.

(E) RT–qPCR analysis of knockdown efficiency of MYH9 and MYH10 in HCT116 cells.

(F) RT–qPCR analysis of YAP target genes (*CTGF, THBS1,* and *NUAK2*) in HCT116 NC and shMYH9 cells treated under normal conditions, GD or GD supplemented with G.

(G) Immunoblotting of LATS1 distribution in the supernatants and pellets separated after incubating the cell lysates with the indicated concentrations of D5P. G3BP1 or Tubulin was used as a loading control.

(H) Immunoblotting analysis of the effect of MST1/2 inhibitor (XMU-MP-1) on GD-induced YAP activation in HCT116 cells. Actin was used as a loading control.

(I) Immunoblotting analysis of the effect of F-actin dysregulation by CDC42 inhibitor MBQ167 or CDC42BPA depletion on GD-induced YAP activation in HCT116 cells. Tubulin or actin was used as a loading control.

Figure S5: YAP activity influences purine nucleoside metabolism

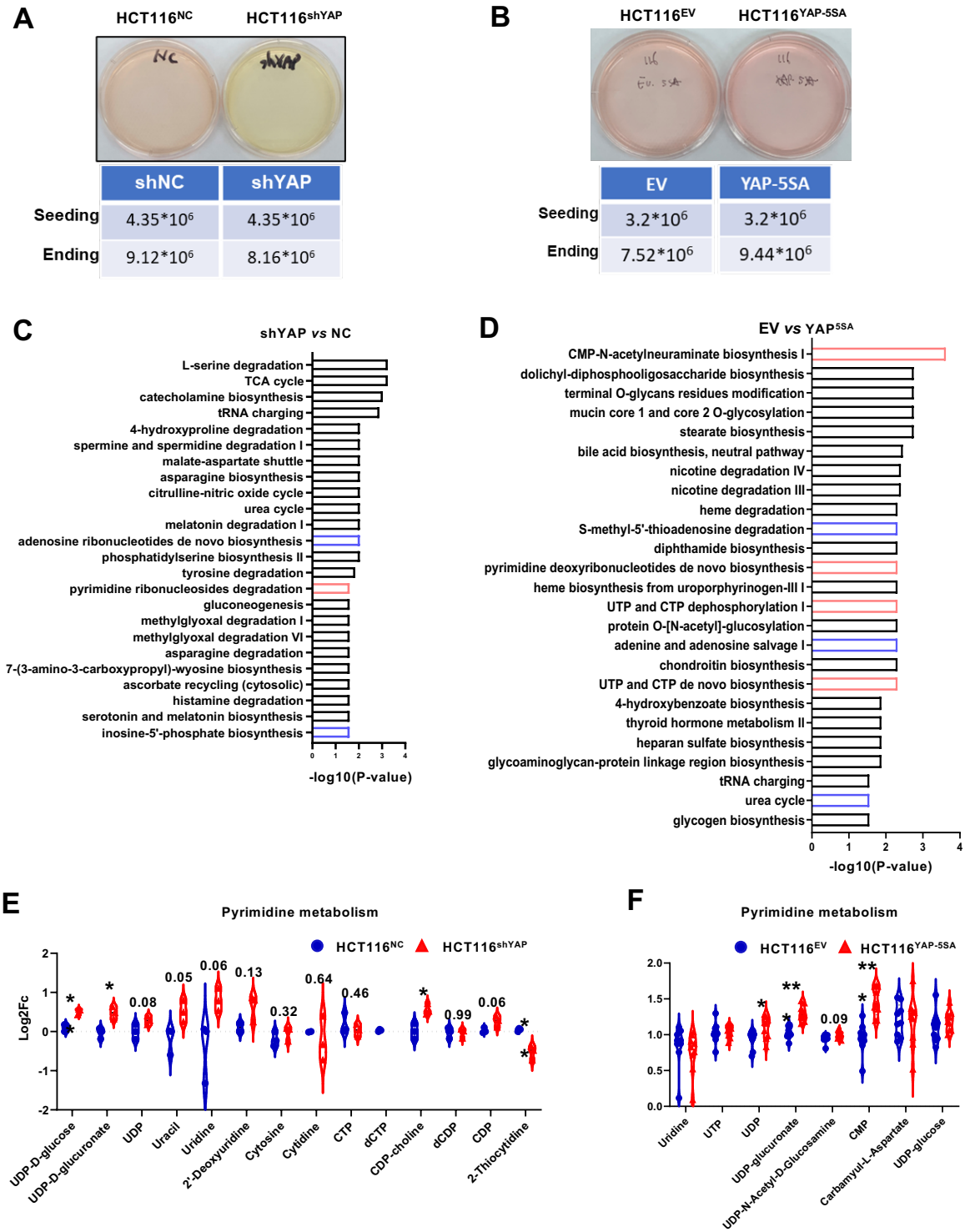

Figure. S5. YAP activity influences purine nucleoside metabolism. Related to Figure 5.

(A) Representative images of HCT116 NC cells and shYAP cells showing the different intensities of medium acidification.

(B) Representative images of HCT116 EV cells and YAP-5SA cells showing the different intensities of medium acidification.

(C) Metabolite set enrichment of the polar metabolites from HCT116 shYAP cells vs. NC cells.

(D) Metabolite set enrichment of the polar metabolites from HCT116 YAP-5SA cells vs. EV cells. Pathways associated with pyrimidine metabolism and purine metabolism are marked in red and blue, respectively.

(E) Relative levels of metabolites involved in pyrimidine nucleotide metabolism in HCT116 NC cells and shYAP cells.

(F) Relative levels of metabolites involved in pyrimidine nucleotide metabolism in HCT116 EV cells and YAP-5SA cells.

Figure S6: YAP deficiency reprograms GD-induced metabolic changes

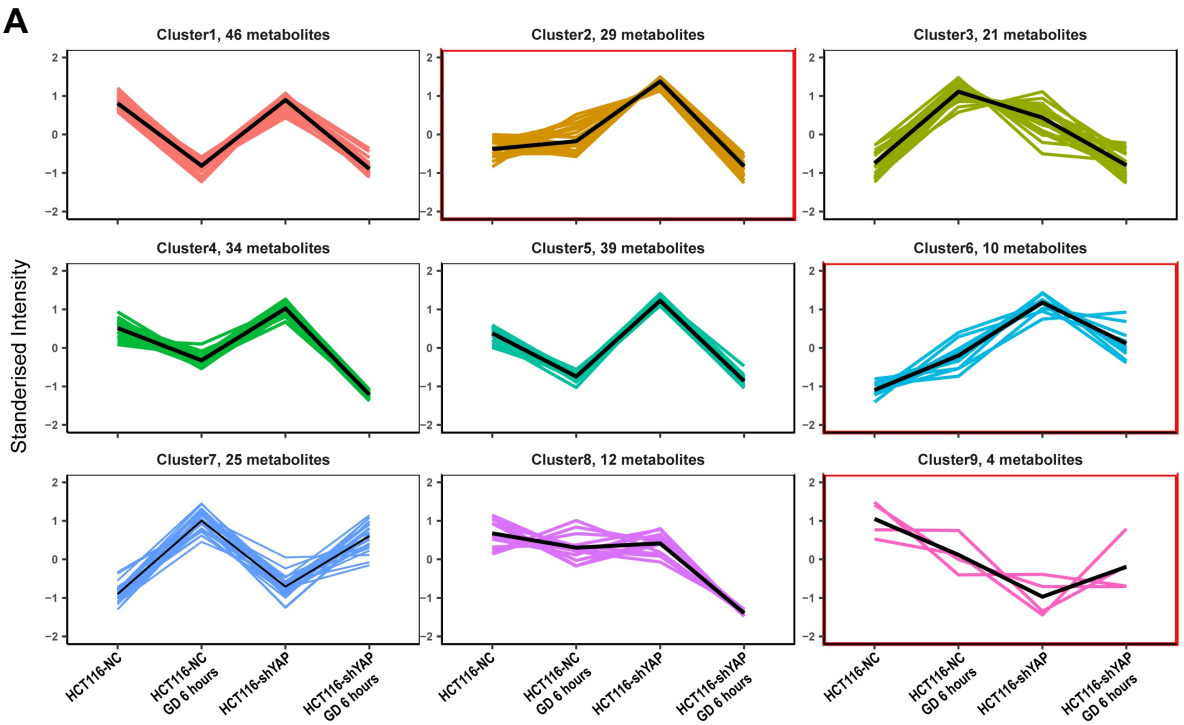

Figure. S6. YAP deficiency reprograms GD-induced metabolic changes. Related to Figure 5.

(A) Cluster analysis of polar metabolite abundance in HCT116 NC cells and shYAP cells under normal conditions or GD (0 mM, 6 h).

Figure S7: PNP-D5P axis is negatively associated with YAP signaling

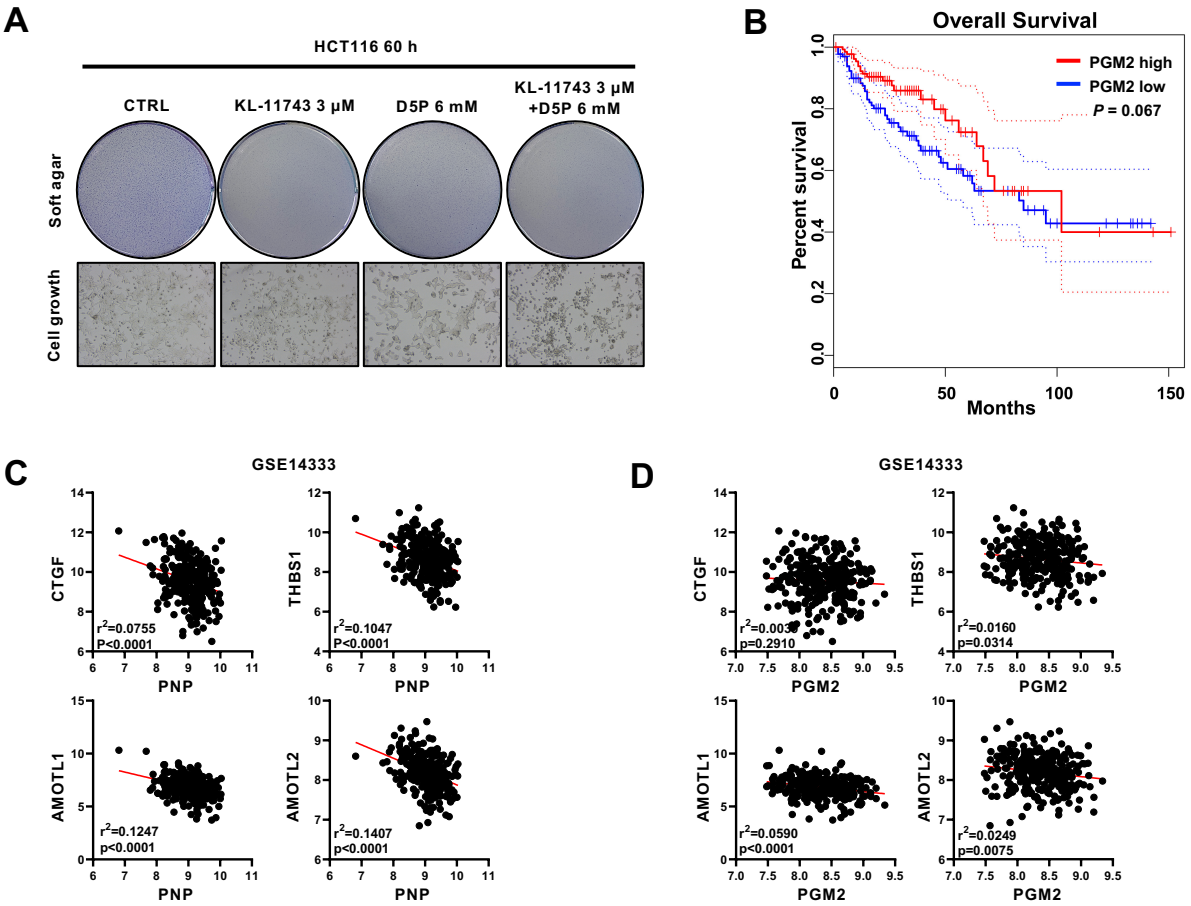

Figure. S7. PNP-D5P axis is negatively associated with YAP signaling. Related to Figure 6 and Figure 7.

(A) Representative images of soft agar colony formation assays or cell growth observations in HCT116 cells treated with KL-11743 supplemented with or without D5P (60 h).

(B) Kaplan-Meier survival analysis of colon adenocarcinoma patients stratified by PGM2 expression.

(C) Scatter plots showing the correlation between *PNP* and YAP target genes in human CRC (GSE14333).

(D) Scatter plots showing the correlation between *PGM2* and YAP target genes in human CRC (GSE14333).

Figure S8: Results related to Discussion

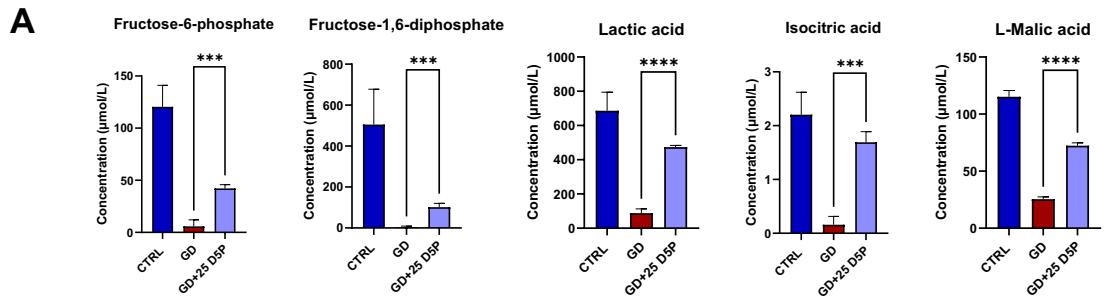

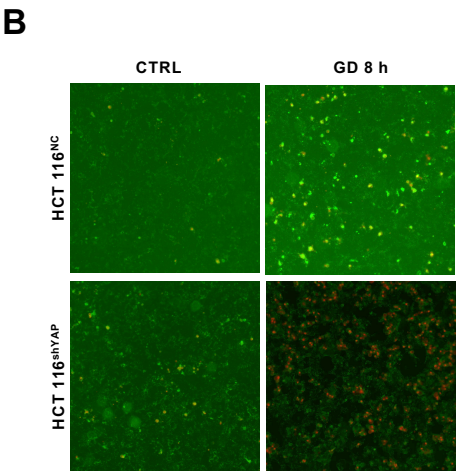

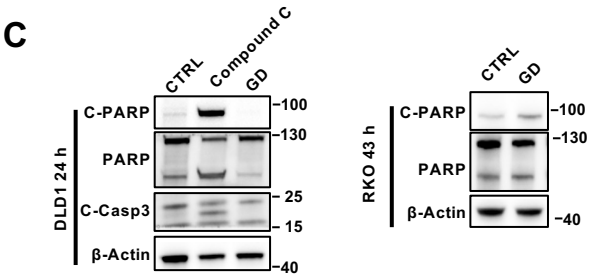

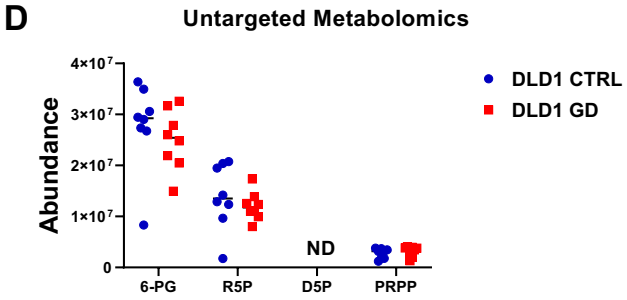

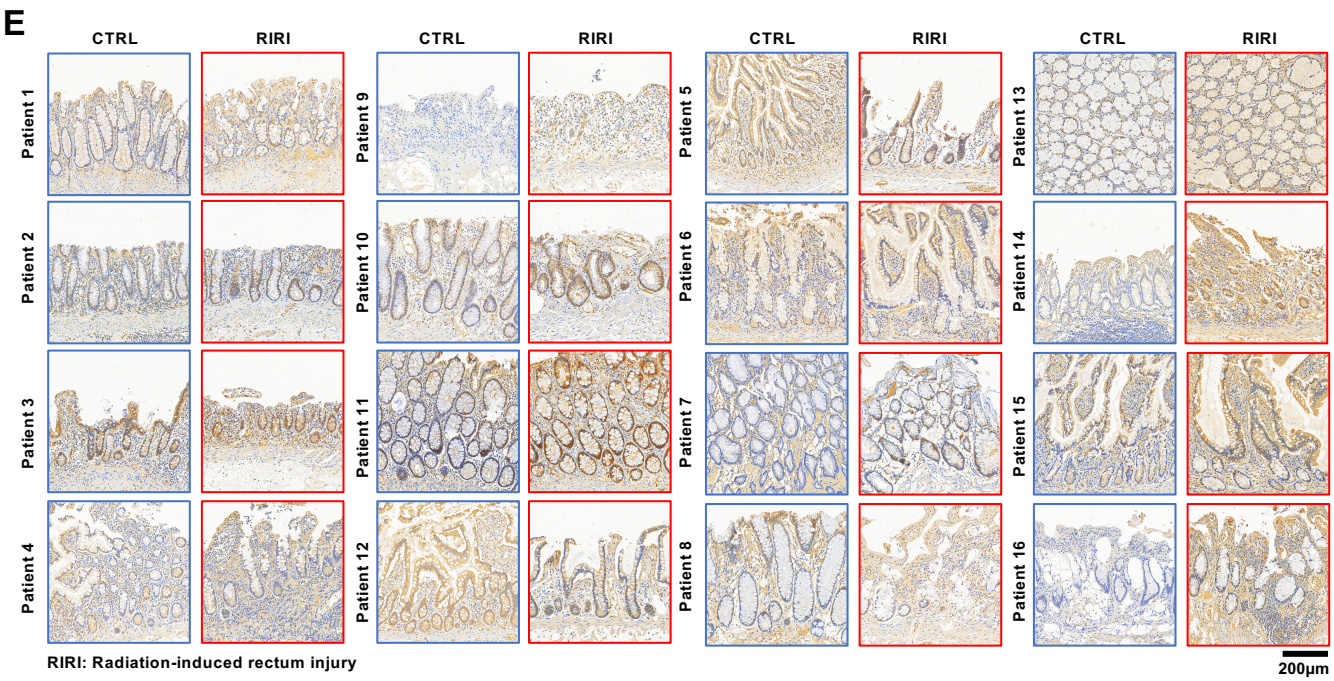

Figure. S8. Results related to Discussion

(A) Relative levels of metabolites involved in glucose metabolism in GD-treated HCT116 cells with or without D5P supplementation.

(B) FITC-Annexin V (green) and PI (red) staining of $HCT116^{NC}$ and $HCT116^{shYAP}$ cell with or without GD treatment.

(C) Immunoblotting analysis of cell death marker in DLD1 and RKO cell with or without GD treatment. Compound C was used a positive control for inducing cell death. β-Actin was used as a loading control.

(D) Metabolic analysis of the metabolites in pentose phosphate pathway in DLD1 cells with or without GD treatment (6-PG: 6-Phosphogluconic acid; R5P: Ribulose 5-phosphate; D5P: D-Ribose-5-phosphate, PRPP: 5-Phospho-alpha-D-ribose 1-diphosphate).

(E) IHC analysis of PNP expression in paired tissues with or without radiation-induced rectum injury.